AST3100 Astrophysical transients

“You don’t observe the same Universe twice!”

Ziggy Pleunis
Meeting 1 Week 9
2022 November 17

📷 X-ray:
NASA/CXC/GSFC/
B.Williams et al;
Optical: DSS

Helium flash

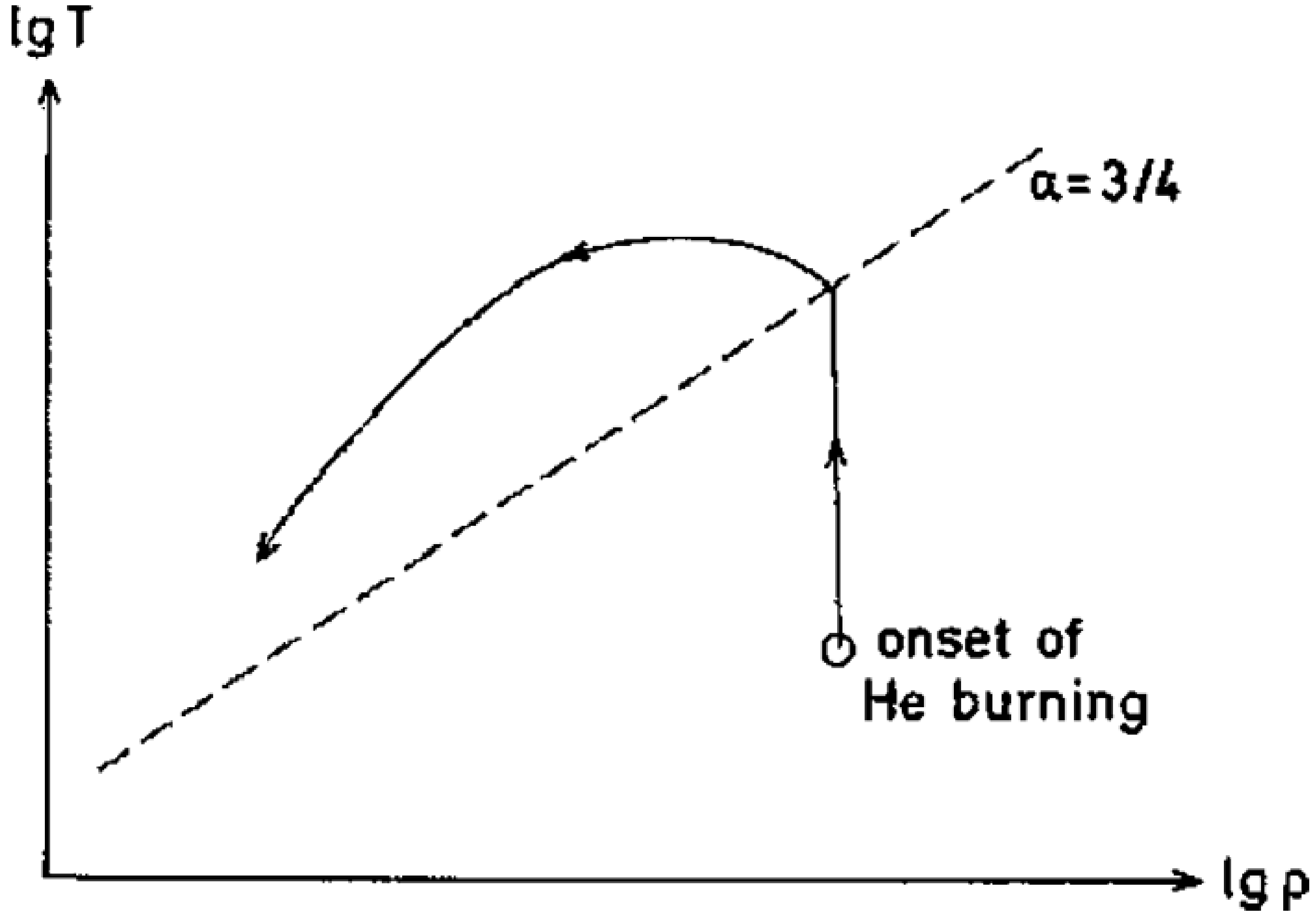

Fig. 33.6 Schematic sketch of the changes of temperature and density during the helium flash. After the ignition temperature is reached in the regime of degeneracy the temperature rises almost without a change of density until degeneracy is removed near the *broken line*. Then a phase of almost isothermal expansion ensuesfollowed by a phase of stable helium burning in the non-degenerate regime

Kippenhahn, Weigert & Weiss 2012

Helium flash

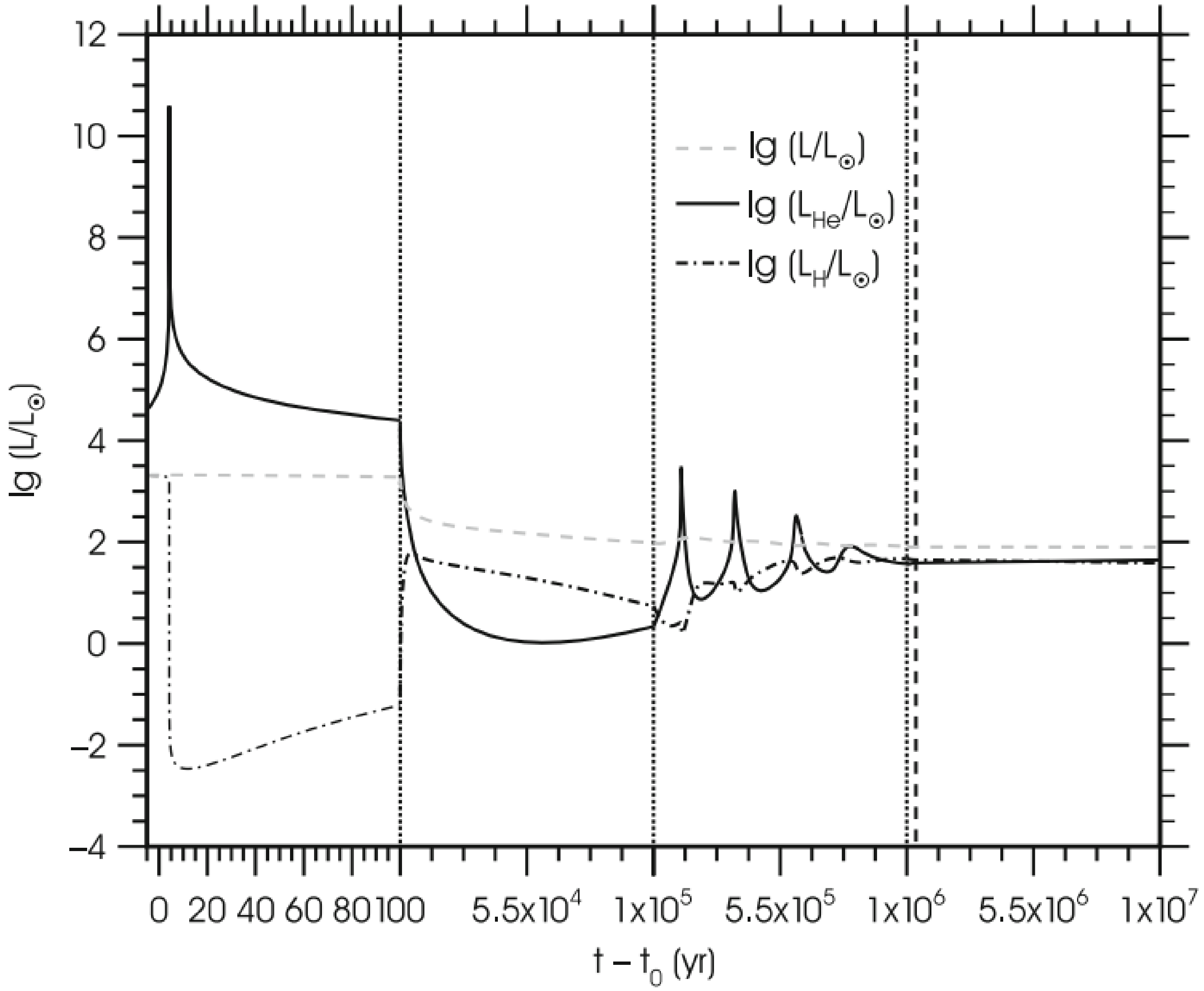

Fig. 33.9 Changes in total (L), hydrogen (L_H), and helium (L_{He}) luminosity with time during the helium flash in the 0.85 $M_\odot$ star of Fig. 33.5. $t = 0$ is defined for the moment when $L_{He}/L_\odot = 5$, and the zero-age horizontal branch is reached 1.325×10^6 years later. This is defined as the point of minimal total thermal energy and indicated by the *vertical dashed line*. *Vertical dotted lines* delimit ranges of different scale for the time axis

Kippenhahn, Weigert & Weiss 2012

Dynamical instability

Fig. 36.1 Schematic evolution of the central values T_0 (in K) and ϱ_0 (in g cm^{-3}) for different core masses. The *dot-dashed line* corresponds to the left-hand part of the *dot-dashed line* in Figs. 28.1 and 28.2. Five evolutionary tracks are plotted which illustrate the different cases discussed in the text: *A* and *B* correspond to case 1. *B** illustrates case 2, where the core gains mass after it has become degenerate and undergoes a carbon flash. The curves *C*, *D* correspond to case 3, while curve *E* corresponds to case 4

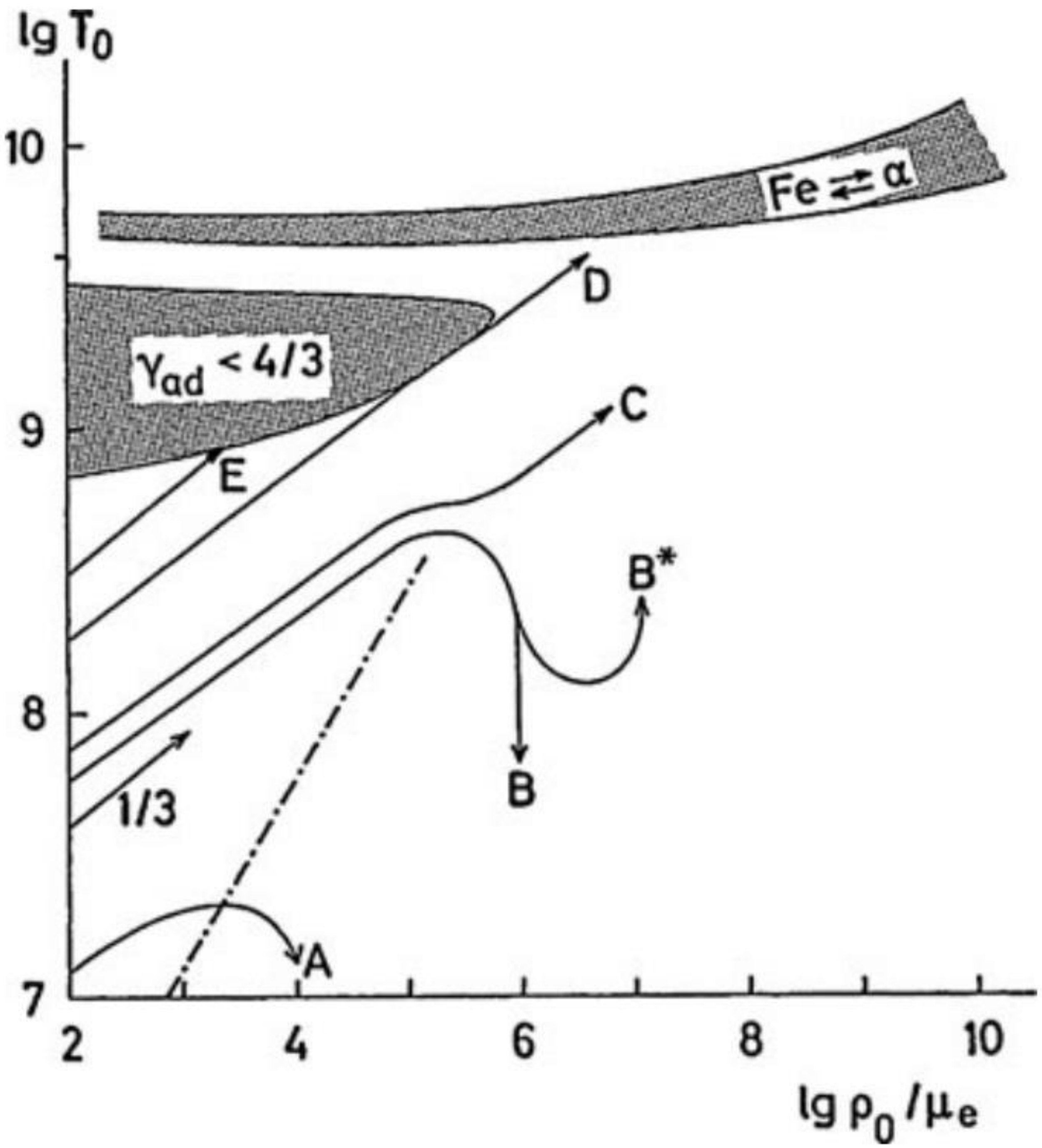

Kippenhahn, Weigert & Weiss 2012

Pair-instability supernovae

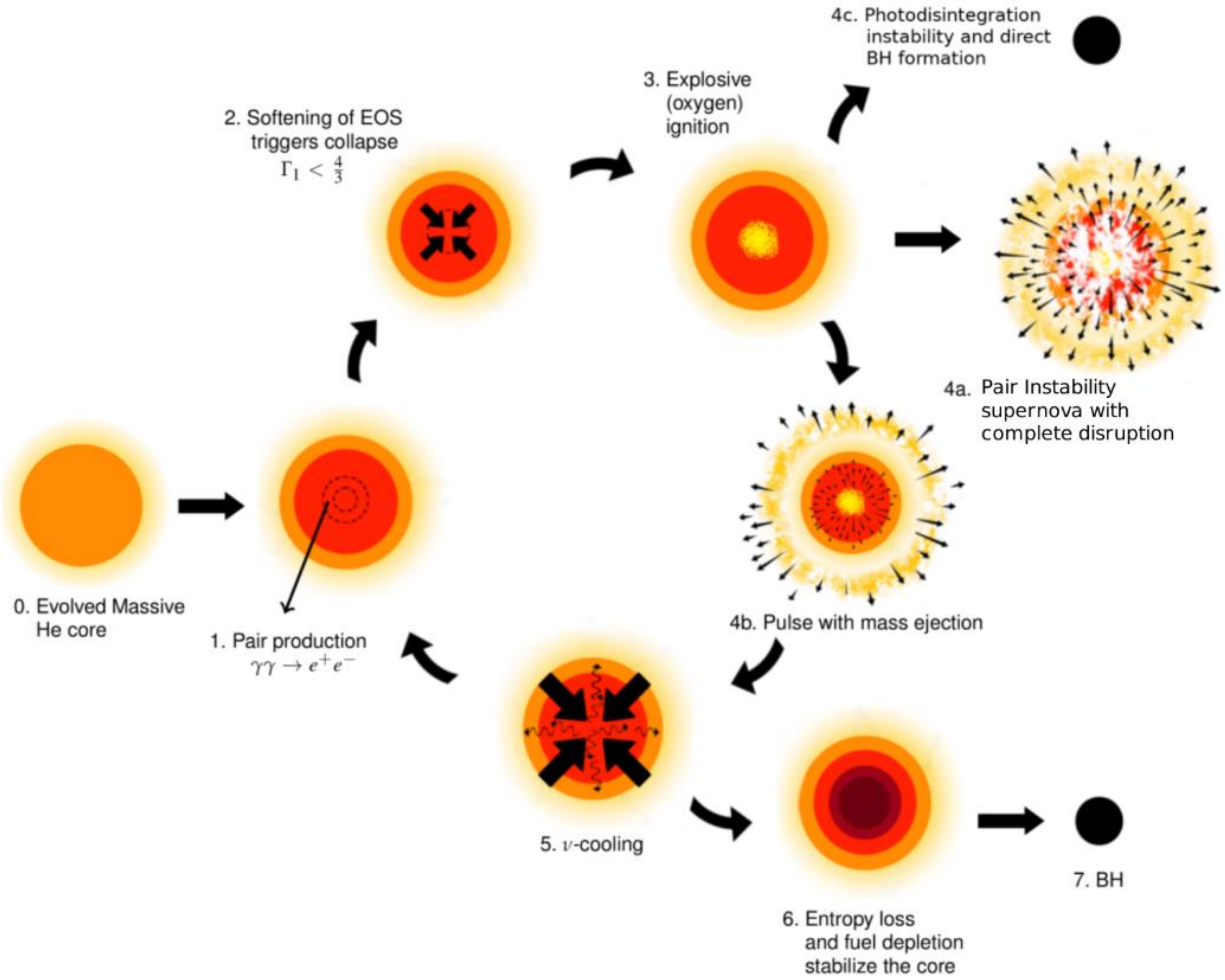

Fig. 1. Evolution of a massive He core undergoing (pulsational) pair instability evolution. Three final outcomes are possible: full disruption without a compact remnant (4a.), formation of a BH because of the photodisintegration instability (4c.), or episodic mass loss (4b.) and final stabilization of the core, followed by a regular core-collapse event.

Renzo+ 2020

Pair-instability supernovae

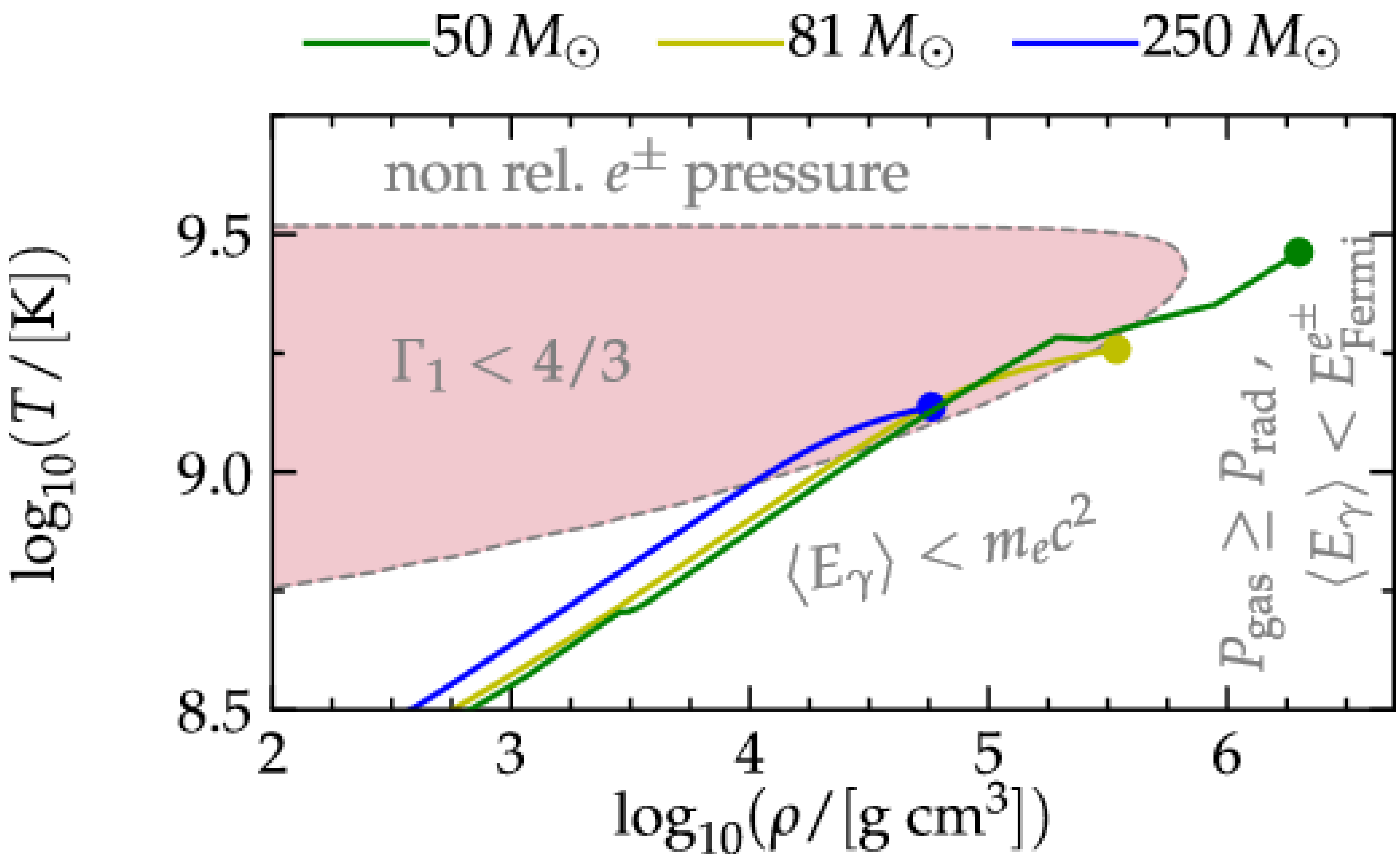

Renzo+ 2020

“How massive single stars end their life”

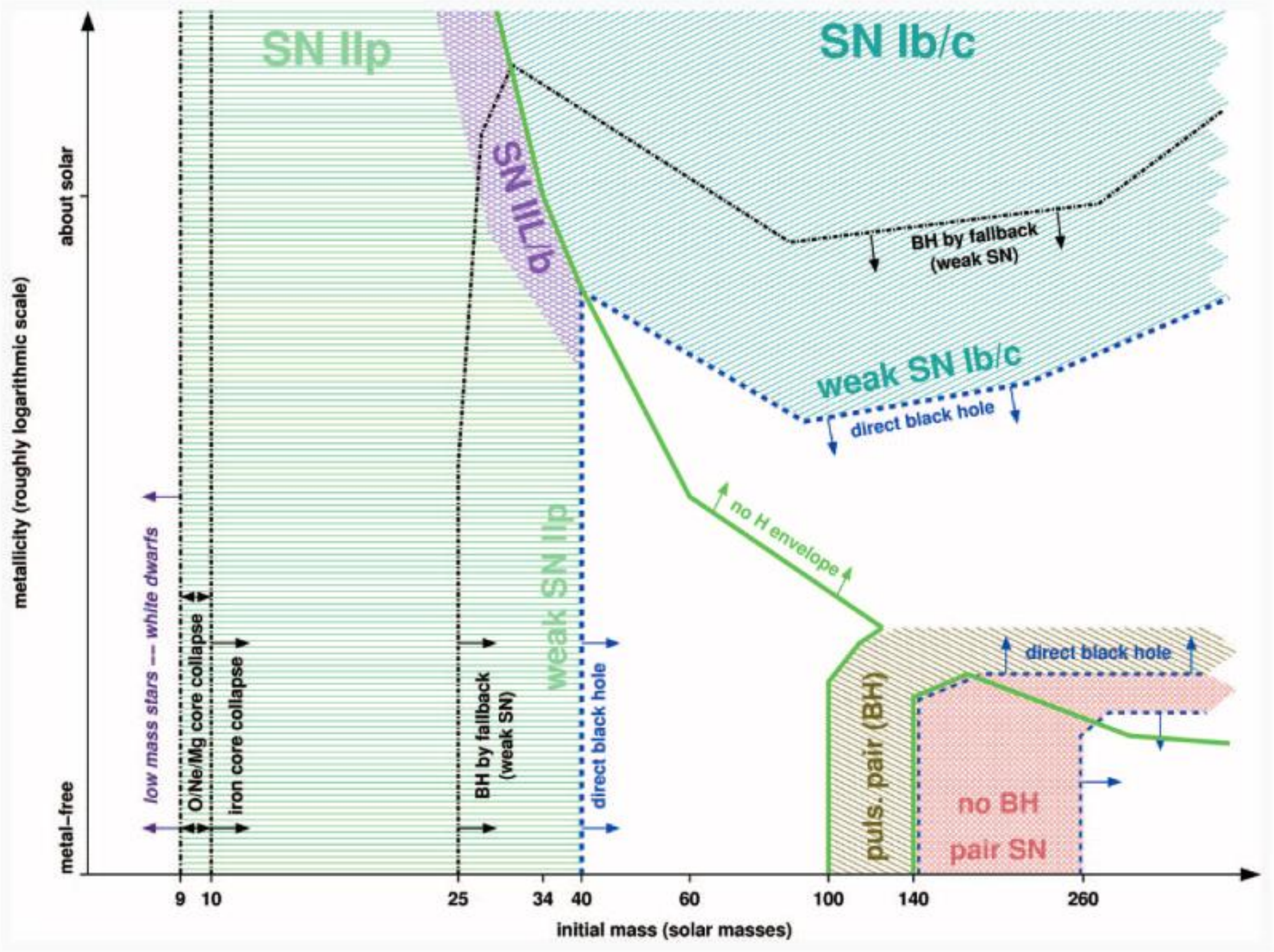

FIG. 2.—Supernovae types of nonrotating massive single stars as a function of initial metallicity and initial mass. The lines have the same meaning as in Fig. 1. Green horizontal hatching indicates the domain where Type IIp supernovae occur. At the high-mass end of the regime they may be weak and observationally faint because of fallback of ^{56}Ni. These weak SN Type IIp should preferentially occur at low metallicity. At the upper right-hand edge of the SN Type II regime, close to the green line of loss of the hydrogen envelope, Type IIL/b supernovae that have a hydrogen envelope of $\lesssim 2\ M_\odot$ are made (*purple cross-hatching*). In the upper right-hand quarter of the figure, above both the lines of hydrogen envelope loss and direct black hole formation, Type Ib/c supernovae occur; in the lower part of their regime (middle of the right half of the figure) they may be weak and observationally faint because of fallback of ^{56}Ni, similar to the weak Type IIp SNe. In the direct black hole regime no “normal” (non–jet-powered) supernovae occur since no SN shock is launched. An exception are pulsational pair-instability supernovae (lower right-hand corner; *brown diagonal hatching*) that launch their ejection before the core collapses. Below and to the right of this we find the (nonpulsational) pair-instability supernovae (*red cross-hatching*), making no remnant, and finally another domain where black hole are formed promptly at the lowest metallicities and highest masses (*white*) where nor SNe are made. White dwarfs also do not make supernovae (*white strip at the very left*).

Heger+ 2003

Pair-instability supernovae

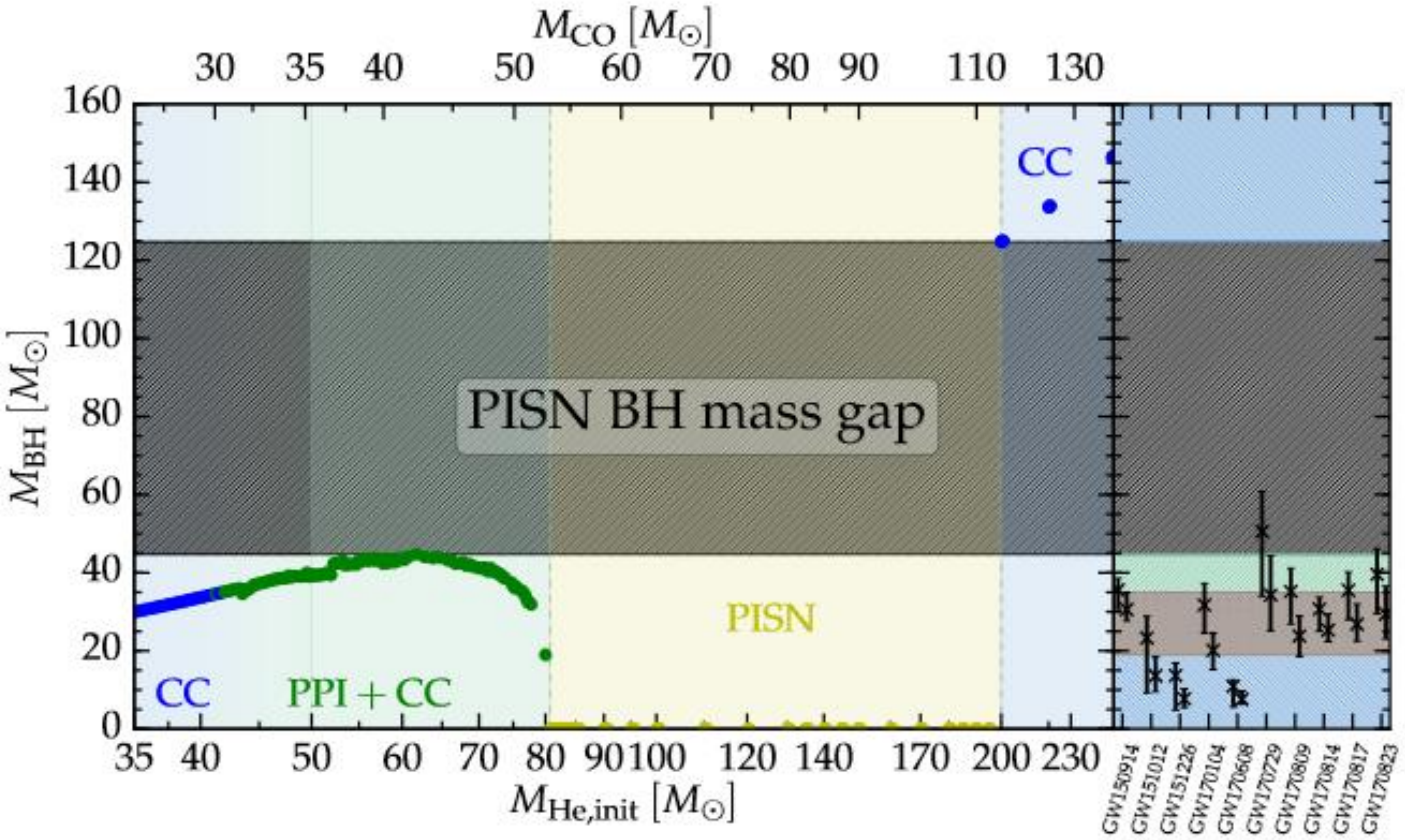

Fig. 2. Final BH masses as a function of the initial He core mass. The scale in the horizontal direction is logarithmic. The colors in the background indicate the approximate range for each evolutionary path, see also Sect. 3. *Right panel*: masses inferred from the first ten binary BH mergers detected by LIGO/Virgo, with a red shade to emphasize the overlap between PPI and CC, and green and blue hatches to indicate the fate of the progenitor in different BH mass ranges.

Renzo+ 2020

Pulsational pair-instability supernovae

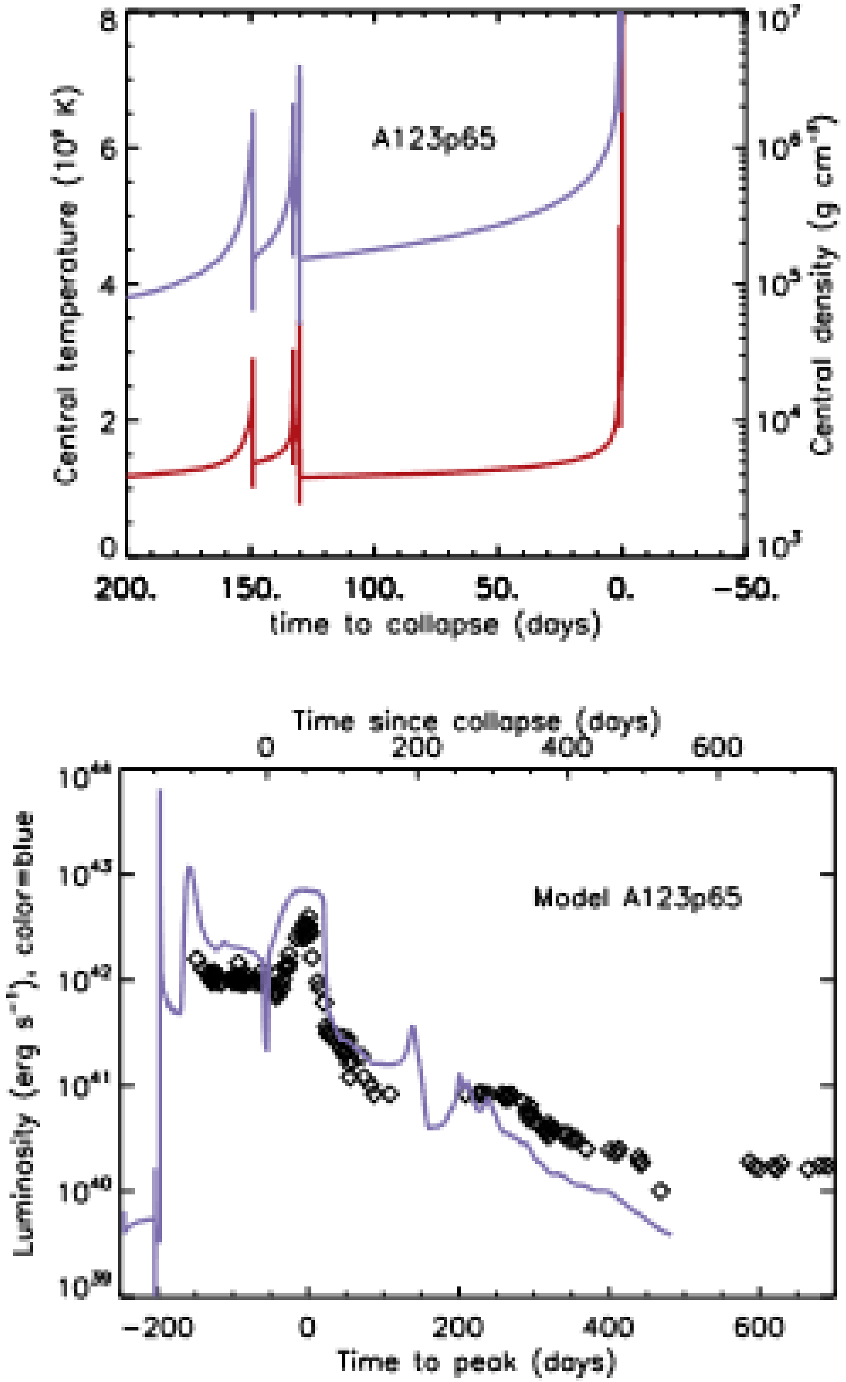

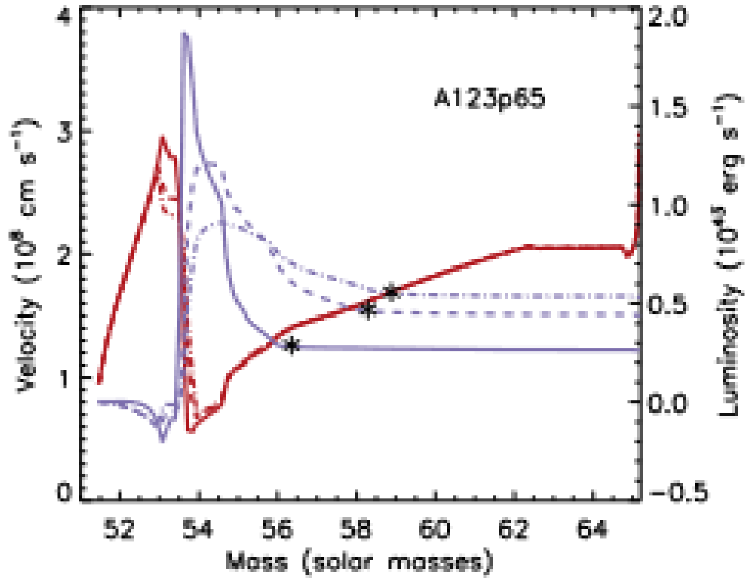

Figure 6. Top: pulsing history of model A123p65. The central temperature (solid red line) and density (solid blue line) are shown as a function of time to core collapse. A weak pulse ($T_p = 2.91$ GK) at 149.1 days before collapse launches a shock that unbinds most of the envelope. Two stronger, closely separated pulses at 132.8 days ($T_p = 3.05$ GK) and 130.3 days ($T_p = 3.46$ GK) illuminate the previously ejected material. Finally, a series of three rapid pulses of 0.977, 0.958, and 0.925 days ($T_p = 4.04$, 4.25, and 4.86 GK) lead to a terminal brightening just as the core collapses to a black hole (the brightening is delayed from the time of pulses because of diffusion time). Middle: comparison of the bolometric light curve of model A123p65 with that estimated for SN 1961V. Time is plotted relative to the observed peak for SN 1961V on the bottom axis and to core collapse on the top axis. The single observed point at −366 days is omitted in this plot, as are observations beyond 700 days post-peak. Bottom: radiation transport in model A123p65. The velocity (red) and luminosity (blue) are shown as a function of mass for three different times, 10 days (solid), 20 days (dashed), and 25 days (dashed–dotted) after core collapse (see the timescale on the top of the middle panel). Note the diffusion of light ahead of the shock. Asterisks indicate the location of the electron scattering photosphere.

Woosley & Smith 2022